



Methanolysis of *Jatropha curcas* Oil for Biodiesel Production

GAJANAN SAHU^{1,2}, S. SAHA¹, SUDIP MAITY³, RAJA SEN¹, S. DATTA¹, PRAKASH CHAVAN¹, B.K. SHARMA¹ and S.N. NAIK^{2,*}

¹Gasification and Fuel Science Division, Central Institute of Mining & Fuel Research (CSIR), Dhanbad-828 108, India

²Centre for Rural Development & Technology, Indian Institute of Technology, Delhi Hauz Khas, New Delhi-110 016, India

³Chemical & Liquid Fuel Division, Central Institute of Mining & Fuel Research (CSIR), Dhanbad-828 108, India

*Corresponding author: Fax: +91 11 26591121; Tel: +91 11 26591162; E-mail: snn@rdat.iitd.ac.in

(Received: 27 August 2010;

Accepted: 18 April 2011)

AJC-9816

The transesterification of jatropha oil with methanol to methyl ester was carried out using $\text{KNO}_3/\text{Al}_2\text{O}_3$ as a solid base catalyst. It was found that the catalyst with 35 % KNO_3 loading and calcined at 773 K showed the optimum condition. When the transesterification was carried out at 70 °C, with a 15:1 molar ratio of methanol to jatropha oil, a reaction time of 7 h and a catalyst amount of 6 % wt, the conversion of jatropha oil was 86 %. The catalyst was also characterized with FTIR, XRD, Brunauer-Emmett-Teller surface area, true density, particle size analyzer and SEM study.

Key Words: Methanolysis, Transesterification, *Jatropha curcas* oil, $\text{KNO}_3/\text{Al}_2\text{O}_3$ catalyst.

INTRODUCTION

Increasing environmental concern such as air pollution, decreasing petroleum fuels reserves, Biodiesel, consisting of fatty acid alkyl esters has been the focus as an alternative renewable fuel. Biodiesel derived from oil and animal fats is used in diesel engine to reduce the dependence of fossil fuel and hence to reduce the air pollution. The common method for biodiesel production is based on the transesterification of vegetable oil and alcohol with homogeneous catalyst. However, homogeneous catalyst has many disadvantages such as difficulty in production separation, large amount of water required for removes the impurities, glycerol and catalyst present in the organic phase. To overcome such problem, environment friendly heterogeneous catalyst is used for biodiesel production due to easy separation of catalyst from the reaction product and eliminating the additional processing cost related with homogeneous catalyst. Heterogeneous catalyst can be anticipated to provide higher catalyst activity, selectivity and longer catalyst life times¹⁻⁶.

Different types of heterogeneous catalysts have been developed for the transesterification of vegetable oil with methanol. For example, Xie *et al.*⁷ reported conversion of 96 % for the transesterification of soybean oil using $\text{KI}/\text{Al}_2\text{O}_3$ as a catalyst under the optimum reaction conditions and also correlated the catalyst activity for the transesterification reaction with its basicity. Kim *et al.*⁸ developed a solid superbase of

$\text{Na}/\text{NaOH}/\gamma\text{-Al}_2\text{O}_3$ which showed almost the same catalytic activity under the optimum reaction condition as that of the conventional homogeneous NaOH catalyst. Gandia *et al.*^{9,10} studied the methanolysis of sunflower oil using alkaline and alkaline-earth metals compounds as a catalysts and also investigated the synthesis of sunflower biodiesel with NaOH/alumina catalyst. Xie *et al.*¹¹ also showed the maximum conversion of 87 % for the transesterification of soybean oil to methyl ester catalyzed by $\text{KNO}_3/\text{Al}_2\text{O}_3$ as a solid base catalyst under the optimum reaction condition of 15:1 molar ratio of methanol to soybean oil, 6.5 % of catalyst amount, 7 h of reaction time and methanol reflux temperature. Granados *et al.*¹² have been studied the biodiesel production from sunflower oil by using activated calcium oxide as a solid base heterogeneous catalyst. Transesterification of rapeseed oil with methanol using heterogeneous base catalyst for biodiesel production have been studied by Kawashima *et al.*¹³. Xie *et al.*¹⁴ achieved the 85.6 % maximum conversion of soybean oil to methyl ester using NaX zeolites loaded with KOH as a heterogeneous catalyst. Boskovic *et al.*¹⁵ have been studied the kinetics of biodiesel synthesis from sunflower oil using CaO heterogeneous catalyst and obtained 91 % maximum conversion. Kontominas *et al.*¹⁶ have been prepared Mg-Al hydrotalcite and K^+ impregnated zirconia catalyst for the transesterification of rapeseed oil and compared the biodiesel with homogeneous catalyst.

In present study, $\text{KNO}_3/\text{Al}_2\text{O}_3$ solid base catalyst was prepared for the transesterification of *Jatropha curcas* oil. The catalyst efficiency in methanolysis of *Jatropha curcas* oil was estimated regarding the jatropha oil conversion to methyl esters. Brunauer-Emmett-Teller SA, XRD, FTIR, true density, SEM, particle size analyzer were employed for catalyst characterization. The effect of the reaction variables such as the molar ratio of methanol to oil, reaction time and the catalyst amount on the conversion of jatropha oil was also investigated.

EXPERIMENTAL

Preparation of the catalyst: The catalyst was prepared by impregnation method. In this method, an aqueous solution of KNO_3 was added slowly to Al_2O_3 and stirred continuously for 0.5 h. The prepared slurry was kept in desiccator, connected to vacuum pump to open pores of the support. The catalysts was heated in water bath to remove the water content followed by drying in hot-air oven at 120°C overnight. Finally, crushed and the $\text{KNO}_3/\text{Al}_2\text{O}_3$ catalysts was calcined in muffle furnace (500°C) in presence of air¹¹ for 5 h. Al_2O_3 used as a support had a surface area of $128\text{ m}^2/\text{g}$.

Catalyst characterization: The ultracycrometer 1000 (Quantachrome, USA) connected with a temperature controller (Julabo, USA) was used to determine the true density of catalysts by using helium as the probe gas¹⁷. This is based on Archimedes principle of fluid displacement and Boyle's law to determine the volume. Here, the displaced fluid is a gas (helium gas) which can easily penetrate the pores. The density of catalyst was taken as the average of ten consecutive analyses.

DRIFT method was incorporated to identifying the FTIR spectra of samples and DTGS detector was used. FTIR spectra of catalysts were recorded on Perkin-Elmer FTIR system (Spectrum GX model) in the region of $4000\text{--}400\text{ cm}^{-1}$ with 2 cm^{-1} resolution by applying KBr pellet technique (sample to KBr ratio 1:300). Each spectrum was obtained in transmission mode over 50 scans. Background spectra were collected before every sampling. KBr was previously air oven-dried to avoid interferences due to presence of water.

The Brunauer-Emmett-Teller (BET) surface area of the calcined catalyst was measured by using Tristar 3000 surface area analyzer (Micromeritics, USA). The surface area of the samples were determined by using Nitrogen as adsorptive gas at -196°C (liquid nitrogen temperature). The Brunauer-Emmett-Teller surface area was determined from adsorption of nitrogen onto the catalyst surface in a liquid nitrogen bath. Before conducting experiment, all the samples are degassed for 3 h at 150°C . The Brunauer-Emmett-Teller surface area was calculated from adsorption of nitrogen in the relative pressure range of 0.05 to 0.3 bar.

Powder X-ray diffraction (XRD) measurement was done with the help of the D-8 advanced (M/S Bruker AXS, Germany) X-ray diffractometer. Spectra were collected over a 2θ range of $10\text{--}75^\circ$ with a step scan mode (Step size of $0.020/\text{step}$, scan speed of $1\text{ s}/\text{step}$). The XRD phases were identified by search match procedure with the help of JCPDS data bank.

Scanning electron microscopy (SEM) analysis of the catalyst was carried out on ZEISS EVO series scanning electron

microscope model EVO 50. The catalyst was coated with silver sputtering unit. The equipment was accelerated at 20.0 kV to estimate the particle shape and size of the catalyst.

The laser based particle analyzer instrument (Fritsch GmbH Germany) was used to determine the size of the catalyst sample with resolution 62 channels ($9\text{ mm}/254\text{ mm}$). Data was recorded over a measuring range of $10[\mu\text{m}]\text{--}670.07[\mu\text{m}]$ at 20 scans.

Transesterification reaction: Commercial available jatropha oil was purchased from market. The gas chromatogram of fatty acid profile of *Jatropha curcas* oil was presented in Fig. 1. The fatty acid composition consisted of palmitic acid (C16:0) 23.2%, palmitoleic acid (C16:1) 0.8 %, stearic acid (C18:0) 10.9 %, oleic acid (C18:1) 52 %, linoleic acid (C18:2) 9.0 % and arachidic acid (C20:0) 0.4 %. Anhydrous methanol and all standards were purchased from Sigma Aldrich. 50 mL of commercially available *Jatropha curcas* oil and catalyst was taken in a 250 mL one-necked glass flask equipped with a temperature controlled magnetic stirrer and water cooled reflux condenser. Then required amount of methanol was added to the flask. The mixture was stirred vigorously and refluxed at 70°C for 7 h. The transesterification reaction is monitored by TLC, HPLC analysis. The solvent system used for TLC is hexane:diethyl ether: acetic acid in the proportion of 85:15:1. The methyl esters present in the product of the transesterification of jatropha oil were analyzed using HPLC (Perkin-Elmer Series 200) equipped with Refractive Index detector (Shodex RI 71). A sphere-5 C-18 column (Perkin-Elmer Brownlee column, $220 \times 4.6\text{ mm}$ with $5\text{ }\mu\text{m}$ particle size) at 40°C was used for separation of the components with $1\text{ mL}/\text{min}$ flow rate of methanol as carrier solvent. The products of transesterification were diluted upto 20 times with HPLC grade methanol and filtered through $2\text{ }\mu\text{m}$ PTFE syringe filter before HPLC analysis. Each component was quantified by comparing the peak areas with their respective standards.

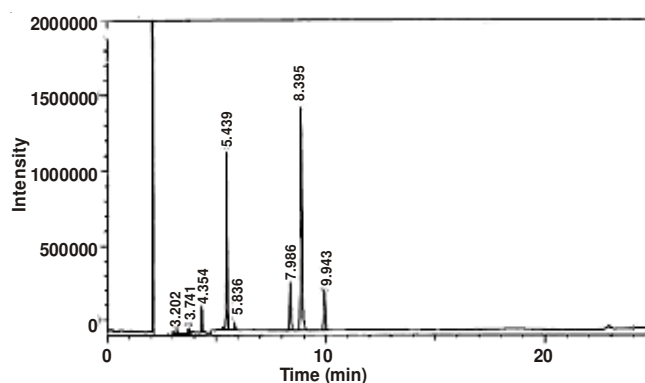


Fig. 1. Gas chromatogram of fatty acids profile of *Jatropha curcas* oil

RESULTS AND DISCUSSION

Catalyst characterizations: Density is one of the important fundamental property of catalyst and useful to provide information regarding their physical and chemical make-up of catalyst. Prior to true density determination of 35 % $\text{KNO}_3/\text{Al}_2\text{O}_3$ catalyst, the catalyst sample was prepared by

removing the atmospheric gases and vapours present in the surface and pores of the catalyst and replacement of these with the probe gas helium. This was performed by purging the sample for 0.5 h. The true density experiment was carried out at 32 °C. The purity of helium gas used was 99.9 %. The true density of 35 % $\text{KNO}_3/\text{Al}_2\text{O}_3$ catalyst was found to be 2.67 g/cc.

The Brunauer-Emmett-Teller surface area of alumina and 35 % $\text{KNO}_3/\text{Al}_2\text{O}_3$ catalyst were found to be 128 and 87.0 m^2/g , respectively. The Brunauer-Emmett-Teller surface area was decreased with loading of potassium nitrate on support. From this result, it was cleared that the introduction of KNO_3 which blocks the pores and reduces the surface area of support. The interactions of the alkali metal compounds with the supports include the formation of solid solution and acid base reaction. The FTIR spectra of 35 % $\text{KNO}_3/\text{Al}_2\text{O}_3$ and Al_2O_3 were shown in Fig. 2. The absorption band at around 1380 cm^{-1} on 35 % $\text{KNO}_3/\text{Al}_2\text{O}_3$ catalyst could be assigned to the vibration of N-O of KNO_3 ¹⁸, while this N-O absorption band was not observed on alumina without loaded KNO_3 . The band of the nitrate on 35 % $\text{KNO}_3/\text{Al}_2\text{O}_3$ catalyst became weaker at higher calcination temperature which result in the decomposition of KNO_3 and formation of K_2O species was observed. The physically absorbed water on the Al_2O_3 and 35 % $\text{KNO}_3/\text{Al}_2\text{O}_3$ catalyst was observed at around 1635 cm^{-1} , attributed to the bending mode of O-H¹⁸. However, the broader band at around 3439 cm^{-1} could be partly assigned to the stretching vibration of Al-O-K group^{19,20}. According to Stork and Pott²¹, on the surface of fully hydroxylated alumina, K^+ ion replaced the protons of isolated hydroxyl groups to form Al-O-K group ($2\text{KNO}_3 + 2\text{Al-OH} \rightarrow \text{N}_2\text{O}_3 + 2\text{Al-O-K} + \text{H}_2\text{O}$), which were considered to be the active basic species. There are many defects or vacancies in the structure of alumina²², resulting from the dehydration of surface hydroxyl groups. So that dispersion of oxide or salt on the alumina is actually the incorporation of potassium ions into the vacancies by strong salt-support interaction or oxide-support interaction. The band at about 1532 cm^{-1} , assigned to carbonates¹¹, was observed on 35 % $\text{KNO}_3/\text{Al}_2\text{O}_3$. This carbonates band were formed by the adsorption of gaseous CO_2 with K_2O species during the calcination procedure in air.

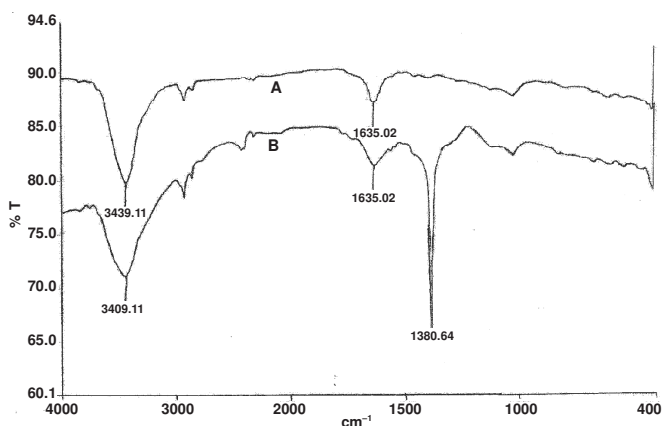


Fig. 2. FTIR spectra of A: Al_2O_3 , B: 35 % $\text{KNO}_3/\text{Al}_2\text{O}_3$

Fig. 3 showed that the XRD pattern of 35 % $\text{KNO}_3/\text{Al}_2\text{O}_3$ catalyst. Based on the diffraction patterns of 35 % $\text{KNO}_3/\text{Al}_2\text{O}_3$ catalyst calcined at 773 K, new characteristics peaks observed

with 2θ of 31, 39, 51, 55 and 62°, which was assigned to K_2O . This K_2O species was the main reason for catalytic activity and basicity of catalyst. The K^+ ions of KNO_3 could insert in the vacant sites of alumina, accelerating dispersion and decomposition of KNO_3 to form strong basic sites of K_2O in the activation process. Thus increase in K_2O species indicate with the increase in the number of basic sites present in the catalyst.

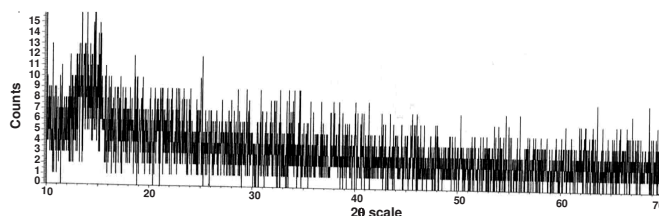


Fig. 3. XRD spectra of 35 % $\text{KNO}_3/\text{Al}_2\text{O}_3$

The scanning electron microscopy of the $\text{KNO}_3/\text{Al}_2\text{O}_3$ catalyst is presented in Fig. 4. It was apparent that most of the SEM photographs of 35 % $\text{KNO}_3/\text{Al}_2\text{O}_3$ sample were the particles of more than 10 μm size and nearly of irregular cluster shape. From the result, it was noticed that a good diffusion of KNO_3 on the surface of Al_2O_3 was observed and therefore the potassium species was found highly distributed upon the surface of the Al_2O_3 support.

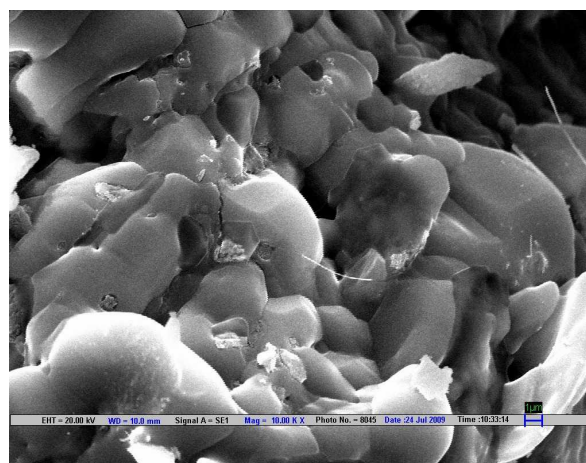


Fig. 4. Scanning electron microscopy image of 35 % $\text{KNO}_3/\text{Al}_2\text{O}_3$

The particle sizes of the catalysts were determined by laser based particle size analyzer (Fritsch GmbH Germany). The laser based particle size analyzer is the most unique and latest modern instrument designed to measure the particle size distribution characteristics of various particles in the range 0.1 to 1250 micron. Particle size measurement is done by analyzing the pattern of scattered light which is produced when particle pass through a laser beam. The particle size distributions of Al_2O_3 and $\text{KNO}_3/\text{Al}_2\text{O}_3$ catalyst have been shown in Figs. 5 and 6, respectively. From these figure, it has been confirmed that most of the particles have large size and the particle size of Al_2O_3 has larger than the particle size of $\text{KNO}_3/\text{Al}_2\text{O}_3$ catalyst. The particle is easy to separate from the reaction product after the transesterification reaction due to bigger size of particle. The same result also obtained from SEM study of the $\text{KNO}_3/\text{Al}_2\text{O}_3$ catalyst.

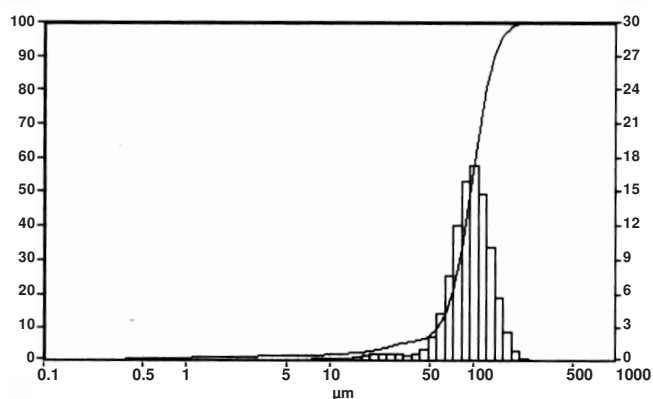


Fig. 5. Particle size distribution of Al_2O_3 catalyst (10.00 % < 57.82 μm , 50.00 % < 97.06 μm , 90.00 % < 141.98 μm)

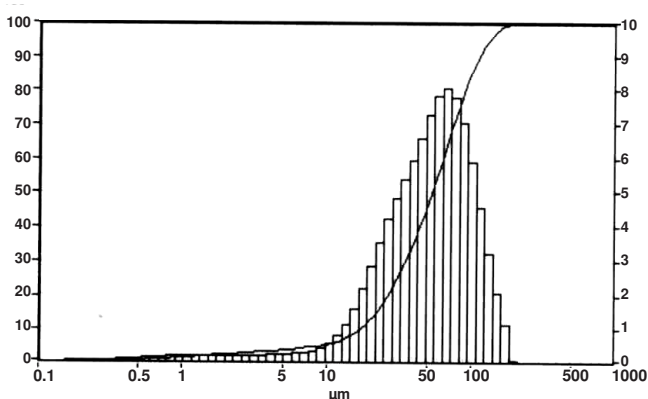


Fig. 6. Particle size distribution of 35 % $\text{KNO}_3/\text{Al}_2\text{O}_3$ catalyst (10.00 % < 17.60 μm , 50.00 % < 54.07 μm , 90.00 % < 113.26 μm)

Taking into consideration of all the information obtained from the catalyst characterizations, it was concluded that K_2O species derived from KNO_3 and the Al-O-K group were the main active sites of the catalyst.

Variable factors affecting the transesterification reaction

Influence of reaction temperature: The transesterification reaction was carried out at different reaction temperature such as 60, 65, 70, 80 and 100 $^\circ\text{C}$. The methanol to oil molar ratio was 15:1 with 6 % $\text{KNO}_3/\text{Al}_2\text{O}_3$ catalyst. Fig. 7 showed the graph of reaction temperature vs. conversion. The conversion of jatropha oil was maximum *i.e.* 86 % when the temperature was 70 $^\circ\text{C}$ and then slightly increases with increase in temperature. It has been shown that the amount of methyl ester was affected with increase or decrease in temperature.

Influence of catalyst amount: The effect of 35 % $\text{KNO}_3/\text{Al}_2\text{O}_3$ catalyst amount on the conversion of *Jatropha curcas* oil was shown in Fig. 8. The catalyst amount was varied in the range of 1.0 to 8.0 %. From Fig. 8, it has been observed that when the catalyst amount increased from 1 to 6 %, the conversion of jatropha oil to methyl esters was increased with 600 rpm. However, with further increase in the catalyst amount the conversion was decreased which was possible due to a mixing effect involving reactants, products and solid catalysts. The maximum conversion upto 86 % was achieved at about 6 % catalyst amount. Wang *et al.*²³ reported the best results

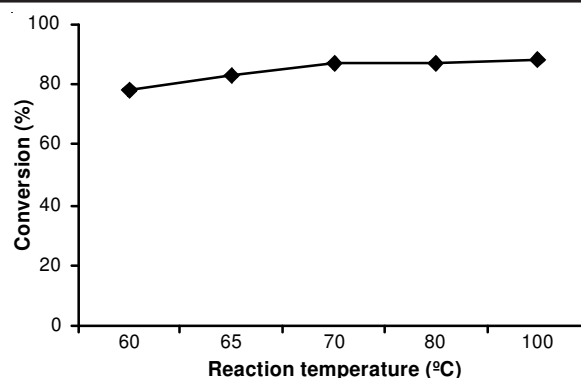


Fig. 7. Influence of reaction temperature on the conversion. Reaction condition: methanol/oil molar ratio 15:1, catalyst amount 6 %, reaction time 7 h and 600 rpm

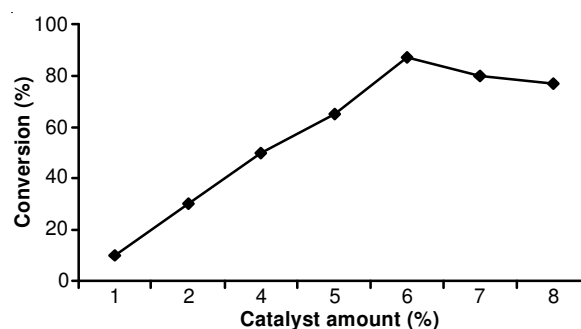


Fig. 8. Influence of catalyst amount on the conversion. Reaction condition: methanol/oil molar ratio 15:1, reaction temperature 70 $^\circ\text{C}$, reaction time 7 h and 600 rpm

for 3 % SrO catalyst amount, 12:1 molar ratio of methanol to oil and 65 $^\circ\text{C}$ while using soybean oil for transesterification reaction.

Influence of molar ratio of methanol to *Jatropha curcas* oil: The conversion of jatropha oil vs. molar ratio of methanol to oil such as 6:1, 8:1, 10:1, 12:1, 15:1 *etc.* are shown in Fig. 9. When the methanol loading amount on molar ratio was increased, the conversion of jatropha oil was increased considerably. When methanol to oil molar ratio was very close to 15:1, the maximum conversion of methyl esters was reached. However, with further increase in the molar ratio there was no significant effect on the conversion. Therefore, the optimum molar ratio of methanol to oil for biodiesel production was approximately 15:1 with 600 rpm. Vyas *et al.*²⁴ reported the maximum 84 % conversion for 12:1 molar ratio of methanol to oil, reaction time 6 h and 70 $^\circ\text{C}$ by using same catalyst for the transesterification of jatropha oil. However, it has been found that the methanol/oil molar ratio 6:1 could give the best conversion when the transesterification reaction was carried out using conventional homogeneous catalyst such as KOH and NaOH ²⁵.

Influence of reaction time: The conversion *versus* reaction time is presented in Fig. 10. It can be observed that the conversion was increased, when the reaction time was raised from 1 to 7 h and thereafter remained unchanged. The maximum conversion was found to be about 86 % at 7 h of reaction time with 600 rpm. Wenlei *et al.*^{7,11} achieved maximum conversion of soybean oil to methyl ester for 8 and 7 h while using $\text{KI}/\text{Al}_2\text{O}_3$ and $\text{KNO}_3/\text{Al}_2\text{O}_3$ as solid base catalyst, respectively.

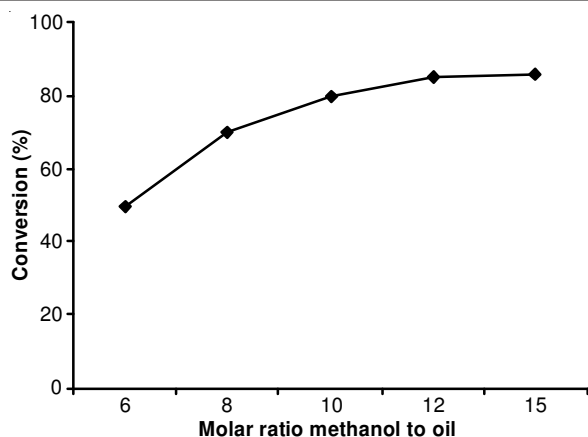


Fig. 9. Influence of molar ratio on the conversion. Reaction condition: catalyst amount 6 %, reaction temperature 70 °C, reaction time 7 h and 600 rpm

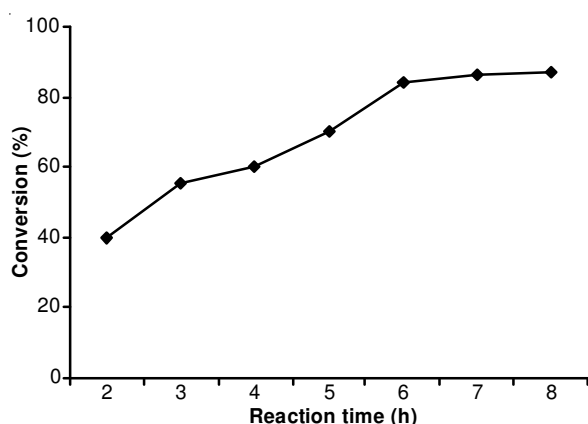


Fig. 10. Influence of reaction time on the conversion. Reaction condition: methanol/oil molar ratio 15:1, catalyst amount 6 %, reaction temperature 70 °C and 600 rpm

Influence of loading amount of KNO₃ on alumina: Fig. 11 showed the plot of loading amount of KNO₃ on alumina versus conversion. When the loading amount of KNO₃ was increased from 15 to 35 wt %, the conversion increased and maximum conversion of 86 % was obtained at loading KNO₃ of 35 wt % on Al₂O₃. However, when the loading amount of

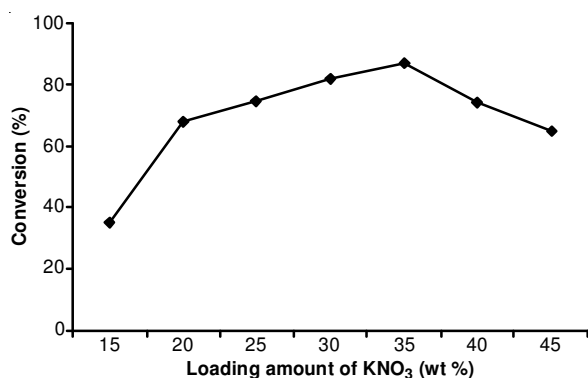


Fig. 11. Influence of loading amount of KNO₃ on the conversion. Reaction condition: methanol/oil molar ratio 15:1, catalyst amount 6 %, reaction temperature 70 °C, reaction time 7 h and 600 rpm

KNO₃ was over 35 wt %, the conversion was decreased. This is due to the excess KNO₃ could cover the basic sites on the surface of catalyst and cause a lowered catalytic activity. Finally it has been observed that the optimum loading amount of KNO₃ was 35 wt %.

Conclusion

Alumina loaded with potassium nitrate, which was prepared by the impregnation of alumina with an aqueous solution of KNO₃ followed by calcination in air, showed high catalytic activities for the transesterification of jatropha oil with methanol. The catalyst with 35 wt % KNO₃ loaded on Al₂O₃ and after calcined at 500 °C for 5 h was found to be optimum catalyst which gave the best catalytic activity for the reaction. When the reaction was carried out at 70 °C, with a molar ratio of methanol to oil of 15:1, a reaction time 7 h and a catalyst amount 6 %, the highest conversion of jatropha oil reached 86 %. Both the K₂O species formed by the thermal decomposition of loaded KNO₃ and the surface Al-O-K groups formed by salt-support interactions were most likely the main reasons for the catalytic activity towards the transesterification reaction.

REFERENCES

1. F. Anwar and U. Rashid, *Fuel*, **87**, 265 (2008).
2. G. Vicente, M. Martinez and J. Aracil, *Bioresour. Technol.*, **92**, 297 (2004).
3. Y.C. Sharma, B. Singh and S.N. Upadhyay, *Fuel*, **87**, 2355 (2008).
4. D.Y.C. Leung and Y. Guo, *Fuel Process. Technol.*, **87**, 883 (2006).
5. M.M. Gui, T.K. Lee and S. Bhatia, *Energy*, **33**, 1646 (2008).
6. N.I. Martyanov and A. Sayari, *Appl. Catal. A: Gen.*, **339**, 45 (2008).
7. X. Wenlei and L. Haitao, *J. Molecul. Catal. A: Chem.*, **255**, 1 (2006).
8. H.J. Kim, B. Kang, M. Kim, Y.M. Park, D. Kim, J. Lee and K.Y. Lee, *Catal. Today*, **93**, 315 (2004).
9. G. Arzamendi, E. Arguinarena, I. Campo, S. Zabala and L.M. Gandia, *Catal. Today*, **133-135**, 305 (2008).
10. G. Arzamendi, E. Arguinarena, I. Campo, M. Sanchez, M. Montes and L.M. Gandia, *Chem. Eng. J.*, **134**, 123 (2007).
11. X. Wenlei, H. Peng and L. Chen, *Appl. Catal. A: Gen.*, **300**, 67 (2006).
12. M.L. Granados, M.D. Zafra Poves, D.M. Alonso, R. Mariscal, F. Galisteo, R. Moreno-Tost, J. Santamaria and J.L.G. Fierro, *Appl. Catal. B: Environ.*, **73**, 317 (2007).
13. A. Kawashima, K. Matsubara and K. Honda, *Bioresour. Technol.*, **99**, 3439 (2008).
14. X. Wenlei, H. Xiaoming and L. Haitao, *Bioresour. Technol.*, **98**, 936 (2007).
15. D. Vujcic, D. Comic, A. Zarubica, R. Micic and G. Boskovic, *Fuel*, **89**, 2054 (2010).
16. K.G. Georgogianni, A.K. Katsoulidis, P.J. Pomonis, G. Manos and M.G. Kontominas, *Fuel Process. Technol.*, **90**, 1016 (2009).
17. S. Saha, B.K. Sharma, S. Kumar, G. Sahu, Y.P. Badhe, S.S. Tambe and B.D. Kulkarni, *Fuel*, **86**, 1594 (2007).
18. K. Nakamoto, *Infrared Spectra of Inorganic and Coordination Compounds*, John Wiley, New York, p. 98 (1970).
19. B.W. Krupay and Y. Amenomiya, *J. Catal.*, **67**, 362 (1981).
20. R.M. Levy and D.J. Bauer, *J. Catal.*, **76**, 345 (1982).
21. W.H.J. Stork and G.T. Pott, *J. Phys. Chem.*, **78**, 2496 (1974).
22. J.B. Peri, *J. Phys. Chem.*, **69**, 220 (1965).
23. L. Xuejun, H. Huayang, W. Yujun and Z. Shenlin, *Catal. Commun.*, **8**, 1107 (2007).
24. A. Vyas, N. Subrahmanyam and P.A. Patel, *Fuel*, **88**, 625 (2009).
25. O.E. Ikwuagwu, I.C. Ononogbu and O.U. Njoku, *Ind. Crops Prod.*, **12**, 57 (2000).